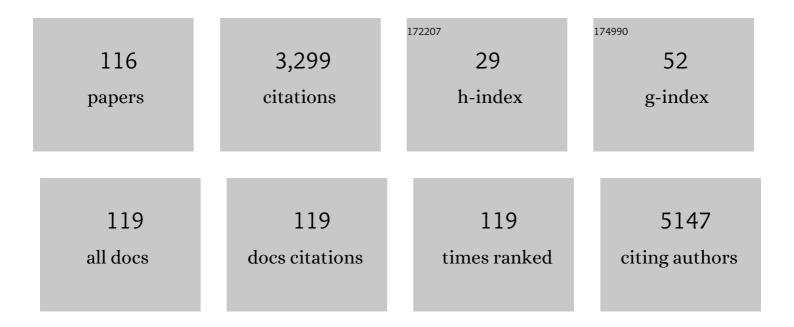
Christopher J Garvey

List of Publications by Year in descending order

Source: https://exaly.com/author-pdf/716086/publications.pdf Version: 2024-02-01



#	Article	IF	CITATIONS
1	Effect of head-group size on micellization and phase behavior in quaternary ammonium surfactant systems. The Journal of Physical Chemistry, 1993, 97, 10236-10244.	2.9	235
2	On the Interpretation of X-Ray Diffraction Powder Patterns in Terms of the Nanostructure of Cellulose I Fibres. Macromolecular Chemistry and Physics, 2005, 206, 1568-1575.	1.1	233
3	Ion transport in complex layered graphene-based membranes with tuneable interlayer spacing. Science Advances, 2016, 2, e1501272.	4.7	203
4	High and Stable Ionic Conductivity in 2D Nanofluidic Ion Channels between Boron Nitride Layers. Journal of the American Chemical Society, 2017, 139, 6314-6320.	6.6	193
5	QUOKKA, the pinhole small-angle neutron scattering instrument at the OPAL Research Reactor, Australia: design, performance, operation and scientific highlights. Journal of Applied Crystallography, 2018, 51, 294-314.	1.9	156
6	Characterization of red-shifted phycobilisomes isolated from the chlorophyll f -containing cyanobacterium Halomicronema hongdechloris. Biochimica Et Biophysica Acta - Bioenergetics, 2016, 1857, 107-114.	0.5	91
7	Superhydrophobic and Superoleophilic Micro-Wrinkled Reduced Graphene Oxide as a Highly Portable and Recyclable Oil Sorbent. ACS Applied Materials & amp; Interfaces, 2016, 8, 9977-9985.	4.0	80
8	A fundamental study on photo-oxidative degradation of linear low density polyethylene films at embrittlement. Polymer, 2012, 53, 2385-2393.	1.8	78
9	A New Insight into Growth Mechanism and Kinetics of Mesoporous Silica Nanoparticles by in Situ Small Angle X-ray Scattering. Langmuir, 2015, 31, 8478-8487.	1.6	78
10	Electroactive properties of electrospun silk fibroin for energy harvesting applications. Nano Energy, 2019, 66, 104106.	8.2	72
11	Just add sugar forÂcarbohydrate induced self-assembly of curcumin. Nature Communications, 2019, 10, 582.	5.8	57
12	Fluid dynamic lateral slicing of high tensile strength carbon nanotubes. Scientific Reports, 2016, 6, 22865.	1.6	53
13	Correlation between Drug Loading Content and Biological Activity: The Complexity Demonstrated in Paclitaxel-Loaded Glycopolymer Micelle System. Biomacromolecules, 2019, 20, 1545-1554.	2.6	53
14	Intrinsically Disordered Stress Protein COR15A Resides at the Membrane Surface during Dehydration. Biophysical Journal, 2017, 113, 572-579.	0.2	51
15	Controlling self-assembly of diphenylalanine peptides at high pH using heterocyclic capping groups. Scientific Reports, 2017, 7, 43947.	1.6	46
16	Shrinkage induced stretchable micro-wrinkled reduced graphene oxide composite with recoverable conductivity. Carbon, 2015, 93, 878-886.	5.4	45
17	Drug-Induced Morphology Transition of Self-Assembled Glycopolymers: Insight into the Drug–Polymer Interaction. Chemistry of Materials, 2018, 30, 5227-5236.	3.2	44
18	Bactericidal activity of self-assembled palmitic and stearic fatty acid crystals on highly ordered pyrolytic graphite. Acta Biomaterialia, 2017, 59, 148-157.	4.1	42

#	Article	IF	CITATIONS
19	Effects of Sugars on Lipid Bilayers during Dehydration â^' SAXS/WAXS Measurements and Quantitative Model. Journal of Physical Chemistry B, 2009, 113, 2486-2491.	1.2	39
20	Localization of trehalose in partially hydrated DOPC bilayers: insights into cryoprotective mechanisms. Journal of the Royal Society Interface, 2014, 11, 20140069.	1.5	39
21	Structural Evolution of Wormlike Micellar Fluids Formed by Erucyl Amidopropyl Betaine with Oil, Salts, and Surfactants. Langmuir, 2016, 32, 12423-12433.	1.6	39
22	Molecular-Scale Understanding of the Embrittlement in Polyethylene Ocean Debris. Environmental Science & Technology, 2020, 54, 11173-11181.	4.6	39
23	Structure and Property Changes in Self-Assembled Lubricin Layers Induced by Calcium Ion Interactions. Langmuir, 2017, 33, 2559-2570.	1.6	38
24	Wormlike micelle formation of novel alkyl-tri(ethylene glycol)-glucoside carbohydrate surfactants: Structure–function relationships and rheology. Journal of Colloid and Interface Science, 2018, 529, 464-475.	5.0	38
25	Thermal fluctuations of haemoglobin from different species: adaptation to temperature via conformational dynamics. Journal of the Royal Society Interface, 2012, 9, 2845-2855.	1.5	37
26	High aspect ratio nanocellulose from an extremophile spinifex grass by controlled acid hydrolysis. Cellulose, 2017, 24, 3753-3766.	2.4	37
27	Changes in microfibril angle in cyclically deformed dry coir fibers studied by in-situ synchrotron X-ray diffraction. Journal of Materials Science, 2008, 43, 350-356.	1.7	35
28	Reversible pH―and Photocontrollable Carbohydrateâ€Based Surfactants. Chemistry - A European Journal, 2014, 20, 13881-13884.	1.7	35
29	Light-induced structural evolution of photoswitchable carbohydrate-based surfactant micelles. Chemical Communications, 2015, 51, 5509-5512.	2.2	35
30	Drug-Directed Morphology Changes in Polymerization-Induced Self-Assembly (PISA) Influence the Biological Behavior of Nanoparticles. ACS Applied Materials & Interfaces, 2020, 12, 30221-30233.	4.0	34
31	Cellulose Dissolution in Ionic Liquid: Ion Binding Revealed by Neutron Scattering. Macromolecules, 2018, 51, 7649-7655.	2.2	31
32	Phospholipid Membrane Protection by Sugar Molecules during Dehydration—Insights into Molecular Mechanisms Using Scattering Techniques. International Journal of Molecular Sciences, 2013, 14, 8148-8163.	1.8	29
33	Biodegradability of Poly-3-hydroxybutyrate/Bacterial Cellulose Composites under Aerobic Conditions, Measured via Evolution of Carbon Dioxide and Spectroscopic and Diffraction Methods. Environmental Science & Technology, 2015, 49, 9979-9986.	4.6	27
34	Sugar Concentration and Arrangement on the Surface of Glycopolymer Micelles Affect the Interaction with Cancer Cells. Biomacromolecules, 2019, 20, 273-284.	2.6	27
35	Effect of deuteration on the phase behaviour and structure of lamellar phases of phosphatidylcholines – Deuterated lipids as proxies for the physical properties of native bilayers. Colloids and Surfaces B: Biointerfaces, 2019, 177, 196-203.	2.5	27
36	Location of sugars in multilamellar membranes at low hydration. Physica B: Condensed Matter, 2006, 385-386, 862-864.	1.3	26

#	Article	IF	CITATIONS
37	The effect of comonomer concentration and distribution on the photo-oxidative degradation of linear low density polyethylene films. Polymer, 2017, 119, 66-75.	1.8	26
38	Direct Comparison of Disaccharide Interaction with Lipid Membranes at Reduced Hydrations. Langmuir, 2015, 31, 9134-9141.	1.6	23
39	Using SANS with Contrast-Matched Lipid Bicontinuous Cubic Phases To Determine the Location of Encapsulated Peptides, Proteins, and Other Biomolecules. Journal of Physical Chemistry Letters, 2016, 7, 2862-2866.	2.1	23
40	Manipulating three-dimensional gel network entanglement by thin film shearing. Chemical Communications, 2016, 52, 4513-4516.	2.2	23
41	Importance of Polymer Length in Fructose-Based Polymeric Micelles for an Enhanced Biological Activity. Macromolecules, 2019, 52, 477-486.	2.2	23
42	Aqueous hydrogen peroxide-induced degradation of polyolefins: AÂgreener process for controlled-rheology polypropylene. Polymer Degradation and Stability, 2015, 117, 97-108.	2.7	22
43	The effects of alkylammonium counterions on the aggregation of fluorinated surfactants and surfactant ionic liquids. Journal of Colloid and Interface Science, 2016, 475, 72-81.	5.0	22
44	Thermal annealing behaviour and gel to crystal transition of a low molecular weight hydrogelator. Soft Matter, 2017, 13, 1006-1011.	1.2	22
45	Measurement of glucose exclusion from the fully hydrated DOPE inverse hexagonal phase. Soft Matter, 2010, 6, 1197.	1.2	21
46	Manipulation of Polyhydroxybutyrate Properties through Blending with Ethyl-Cellulose for a Composite Biomaterial. International Journal of Polymer Science, 2011, 2011, 1-8.	1.2	20
47	Smooth deuterated cellulose films for the visualisation of adsorbed bio-macromolecules. Scientific Reports, 2016, 6, 36119.	1.6	20
48	H2O/D2O Contrast Variation for Ultra-Small-Angle Neutron Scattering to Minimize Multiple Scattering Effects of Colloidal Particle Suspensions. Colloids and Interfaces, 2018, 2, 37.	0.9	20
49	Spontaneous Self-Assembly of Thermoresponsive Vesicles Using a Zwitterionic and an Anionic Surfactant. Biomacromolecules, 2020, 21, 4569-4576.	2.6	20
50	Effect of Polymer Chain Density on Protein–Polymer Conjugate Conformation. Biomacromolecules, 2019, 20, 1944-1955.	2.6	19
51	Phase Behavior, Small-Angle Neutron Scattering and Rheology of Ternary Nonionic Surfactant–Oil–Water Systems: A Comparison of Oils. Langmuir, 2013, 29, 3575-3582.	1.6	18
52	Characterization of porosity in sulfide ore minerals: A USANS/SANS study. American Mineralogist, 2014, 99, 2398-2404.	0.9	18
53	Bio-deuterated cellulose thin films for enhanced contrast in neutron reflectometry. Cellulose, 2017, 24, 11-20.	2.4	18
54	Nacre-bionic nanocomposite membrane for efficient in-plane dissipation heat harvest under high temperature. Journal of Materiomics, 2021, 7, 219-225.	2.8	18

#	Article	IF	CITATIONS
55	Fluorinated lamellar phases: structural characterisation and use as templates for highly ordered silica materials. Soft Matter, 2014, 10, 4902-4912.	1.2	17
56	Picosecond dynamics in haemoglobin from different species: A quasielastic neutron scattering study. Biochimica Et Biophysica Acta - General Subjects, 2014, 1840, 2989-2999.	1.1	17
57	Visualization and Quantification of IgG Antibody Adsorbed at the Cellulose–Liquid Interface. Biomacromolecules, 2017, 18, 2439-2445.	2.6	17
58	The Protein Corona Leads to Deformation of Spherical Micelles. Angewandte Chemie - International Edition, 2021, 60, 10342-10349.	7.2	17
59	Determination of Na+ binding parameters by relaxation analysis of selected23Na NMR coherences: RNA, BSA and SDS. Magnetic Resonance in Chemistry, 2005, 43, 217-224.	1.1	16
60	Phenylene bolaamphiphiles: Influence of the substitution pattern on the aggregation behavior and the miscibility with classical phospholipids. European Journal of Lipid Science and Technology, 2014, 116, 1205-1216.	1.0	16
61	Adsorption of cationic polyacrylamide at the cellulose–liquid interface: A neutron reflectometry study. Journal of Colloid and Interface Science, 2015, 448, 88-99.	5.0	16
62	Photoswitchable Janus glycodendrimer micelles as multivalent inhibitors of LecA and LecB from Pseudomonas aeruginosa. Colloids and Surfaces B: Biointerfaces, 2017, 159, 605-612.	2.5	16
63	The inverse hexagonal – inverse ribbon – lamellar gel phase transition sequence in low hydration DOPC:DOPE phospholipid mixtures. Chemistry and Physics of Lipids, 2009, 157, 56-60.	1.5	15
64	Aggregation behaviour of a single-chain, phenylene-modified bolalipid and its miscibility with classical phospholipids. Beilstein Journal of Organic Chemistry, 2017, 13, 995-1007.	1.3	14
65	Poly(4â€vinyl imidazole): A pHâ€Responsive Trigger for Hierarchical Selfâ€Assembly of Multicompartment Micelles Based upon Triblock Terpolymers. Macromolecular Chemistry and Physics, 2019, 220, 1900131.	1.1	14
66	The morphology of crystallisation of PHBV/PHBV copolymer blends. European Polymer Journal, 2019, 112, 104-119.	2.6	14
67	Small angle scattering in the Porod region from hydrated paper sheets at varying humidities. Holzforschung, 2004, 58, 473-479.	0.9	13
68	The hydration of paper studied with solid-state magnetisation-exchange 1H NMR spectroscopy. Holzforschung, 2006, 60, 409-416.	0.9	13
69	Kinetics of the lamellar gel–fluid transition in phosphatidylcholine membranes in the presence of sugars. Chemistry and Physics of Lipids, 2010, 163, 236-242.	1.5	13
70	Three-Dimensional Organization of Self-Encapsulating <i>Gluconobacter oxydans</i> Bacterial Cells. ACS Omega, 2017, 2, 8099-8107.	1.6	13
71	Structure–property relationships of elementary bamboo fibers. Cellulose, 2016, 23, 3521-3534.	2.4	12
72	Nematic effects and strain coupling in entangled polymer melts under strong flow. Physical Review E, 2016, 94, 020502.	0.8	12

#	Article	IF	CITATIONS
73	Toward the Fabrication of Advanced Nanofiltration Membranes by Controlling Morphologies and Mesochannel Orientations of Hexagonal Lyotropic Liquid Crystals. Membranes, 2017, 7, 37.	1.4	12
74	Investigation of the phase morphology of bacterial PHA inclusion bodies by contrast variation SANS. Physica B: Condensed Matter, 2006, 385-386, 859-861.	1.3	11
75	Biopolymer Deuteration for Neutron Scattering and Other Isotope-Sensitive Techniques. Methods in Enzymology, 2015, 565, 97-121.	0.4	11
76	Assembly of nanoparticles-polyelectrolyte complexes in nanofiber cellulose structures. Colloids and Surfaces A: Physicochemical and Engineering Aspects, 2017, 513, 373-379.	2.3	11
77	Structural Studies of Three-Arm Star Block Copolymers Exposed to Extreme Stretch Suggests a Persistent Polymer Tube. Physical Review Letters, 2018, 120, 207801.	2.9	11
78	Controlling the characteristics of lamellar liquid crystals using counterion choice, fluorination and temperature. Soft Matter, 2015, 11, 261-268.	1.2	10
79	Na + and solute diffusion in aqueous channels of Myverol bicontinuous cubic phase: PGSE NMR and computer modelling. Magnetic Resonance in Chemistry, 2017, 55, 464-471.	1.1	10
80	Impact of Headgroup Asymmetry and Protonation State on the Aggregation Behavior of a New Type of Glycerol Diether Bolalipid. Langmuir, 2018, 34, 4360-4373.	1.6	10
81	Conformational selection of the intrinsically disordered plant stress protein COR15A in response to solution osmolarity – an X-ray and light scattering study. Physical Chemistry Chemical Physics, 2019, 21, 18727-18740.	1.3	10
82	Ultrastructural modeling of small angle scattering from photosynthetic membranes. Scientific Reports, 2019, 9, 19405.	1.6	10
83	Non-reversible heat-induced gelation of a biocompatible Fmoc-hexapeptide in water. Nanoscale, 2020, 12, 8262-8267.	2.8	10
84	Protein-Eye View of the in Meso Crystallization Mechanism. Langmuir, 2019, 35, 8344-8356.	1.6	9
85	Shear-induced alignment of self-associated hemoglobin in human erythrocytes: small angle neutron scattering studies. European Biophysics Journal, 2004, 33, 589-595.	1.2	8
86	Decoupling order and conductivity in doped conducting polymers. Physical Chemistry Chemical Physics, 2016, 18, 19397-19404.	1.3	7
87	Insights into Free Volume Variations across Ion-Exchange Membranes upon Mixed Solvents Uptake by Small and Ultrasmall Angle Neutron Scattering. ACS Applied Materials & Interfaces, 2017, 9, 8704-8713.	4.0	7
88	Deuterated Bacterial Cellulose Dissolution in Ionic Liquids. Macromolecules, 2021, 54, 6982-6989.	2.2	7
89	Quantitative Neutron Dark-Field Imaging of Milk: A Feasibility Study. Applied Sciences (Switzerland), 2022, 12, 833.	1.3	7
90	In vivo deuteration of a native bacterial biopolymer for structural elucidation using SANS. Physica B: Condensed Matter, 2004, 350, E643-E646.	1.3	6

#	Article	IF	CITATIONS
91	In vivo deuteration strategies for neutron scattering analysis of bacterial polyhydroxyoctanoate. European Biophysics Journal, 2008, 37, 711-715.	1.2	6
92	Effect of red blood cell shape changes on haemoglobin interactions and dynamics: a neutron scattering study. Royal Society Open Science, 2020, 7, 201507.	1.1	6
93	Quantitative and structural analysis of isotopically labelled natural crosslinks in type I skin collagen using LC-HRMS and SANS. Journal of Leather Science and Engineering, 2019, 1, .	2.7	6
94	Co-assembly of helical β ³ -peptides: a self-assembled analogue of a statistical copolymer. Pure and Applied Chemistry, 2017, 89, 1809-1816.	0.9	5
95	Phase dependent structural perturbation of a robust multicomponent assembled icosahedral array. Chemical Communications, 2018, 54, 10824-10827.	2.2	5
96	Localisation of alkaline phosphatase in the pore structure of paper. Colloid and Polymer Science, 2017, 295, 1293-1304.	1.0	4
97	Membrane Protein Structures in Lipid Bilayers; Small-Angle Neutron Scattering With Contrast-Matched Bicontinuous Cubic Phases. Frontiers in Chemistry, 2020, 8, 619470.	1.8	4
98	Conformation of poly(ethylene glycol) in aqueous cholinium amino acid hybrid solvents. Journal of Colloid and Interface Science, 2021, 602, 334-343.	5.0	4
99	Small angle neutron scattering on an absolute intensity scale and the internal surface of diatom frustules from three species of differing morphologies. European Biophysics Journal, 2013, 42, 395-404.	1.2	3
100	Micron-scale restructuring of gelling silica subjected to shear. Journal of Colloid and Interface Science, 2019, 533, 136-143.	5.0	3
101	Moisture-activated dynamics on crystallite surfaces in cellulose. Colloid and Polymer Science, 2019, 297, 521-527.	1.0	3
102	Evolution of structural dimensions in mesoporous template precursor from hexagonal lyotropic liquid crystals. Journal of Physics Condensed Matter, 2020, 32, 075101.	0.7	3
103	Coordination crosslinking of helical substituted oligoamide nanorods with Cu(II). Supramolecular Chemistry, 2020, 32, 222-232.	1.5	3
104	Hybrid Nanoparticles for Haloperidol Encapsulation: Quid Est Optimum?. Polymers, 2021, 13, 4189.	2.0	3
105	In Situ SAXS Measurement and Molecular Dynamics Simulation of Magnetic Alignment of Hexagonal LLC Nanostructures. Membranes, 2018, 8, 123.	1.4	2
106	Conformation of Myoglobinâ€Poly(Ethyl Ethylene Phosphate) Conjugates Probed by SANS: Correlation with Polymer Grafting Density and Interaction. Macromolecular Bioscience, 2021, 21, 2000356.	2.1	2
107	The spatial modulation of microfibril angle in the woody tissue of maturing tree stems studied with synchrotron radiation. Australian Journal of Botany, 2020, 68, 267.	0.3	2
108	USANS study of wood structure. Physica B: Condensed Matter, 2006, 385-386, 877-879.	1.3	1

#	Article	IF	CITATIONS
109	THz-TDS of filter paper at differing humidities. , 2010, , .		1
110	The Protein Corona Leads to Deformation of Spherical Micelles. Angewandte Chemie, 2021, 133, 10430-10437.	1.6	1
111	Controlling phase and rheological behaviours of hexagonal lyotropic liquid crystalline templates for nanostructural administration and retention. Journal of Colloid and Interface Science, 2022, 607, 816-825.	5.0	1
112	Comprehensive multidimensional study of the self-assembly properties of a three residue substituted l² ³ oligoamide. Pure and Applied Chemistry, 2021, 93, 1327-1341.	0.9	1
113	Distribution of Solute Molecules in Bilayer Stacks by Medium Angle Diffraction. Biophysical Journal, 2016, 110, 81a.	0.2	0
114	Microstructure characterisation through ultra-small-angle neutron scattering. International Journal of Nanotechnology, 2018, 15, 766.	0.1	0
115	C-amidation of substituted \hat{l}^23 oligoamides yields novel supramolecular assembly motif. Nanotechnology, 2021, 33, .	1.3	0
116	Solid State Polymer Architecture of Empty Fruit Bunches of the African Oil Palm. Reviews and Advances in Chemistry, 2021, 11, 166-177.	0.2	0